Basal Intracellular Free Mg^{2+} Concentration in Smooth Muscle Cells of Guinea Pig Tenia Cecum: Intracellular Calibration of the Fluorescent Indicator Furaptra

Michiko Tashiro and Masato Konishi
Department of Physiology, The Jikei University School of Medicine, Tokyo 105, Japan

ABSTRACT Longitudinal muscle strips dissected from tenia cecum of guinea pig were loaded with the Mg^{2+} indicator, furaptra, and the relation between the fluorescent ratio signal (R) and cytoplasmic free Mg^{2+} concentration ($[Mg^{2+}]_i$) was studied in smooth muscle cells at 25°C. After the application of ionophores (4-bromo-A23187, monensin, and nigericin), a small immediate offset of R (ΔR_{jump}) was followed by a slow change in R (ΔR_{slow}), which reached a steady level within 2–5 h. The ΔR_{jump} was independent of Mg^{2+} concentration in solution ($[Mg^{2+}]_o$), and was thought to be unrelated to the change in $[Mg^{2+}]_i$. The direction of the ΔR_{slow} depended on $[Mg^{2+}]_o$ with a reversal at ~1 mM $[Mg^{2+}]_o$. The intracellular calibration curve was constructed from the steady levels of ΔR_{slow}, and the dissociation constant was 5.4 mM. With the intracellular calibration curve and correction for the ΔR_{jump}, basal $[Mg^{2+}]_i$ was estimated to be 0.98 ± 0.05 mM (mean ± SE, n = 12). When the same calibration was applied to A7r5 cells and rat ventricular myocytes, estimates of basal $[Mg^{2+}]_i$ of these cells were 0.74 ± 0.02 mM (n = 33) and 1.13 ± 0.06 mM (n = 9), respectively. These results suggest that the basal $[Mg^{2+}]_i$ level is ~1 mM at least in some types of smooth muscle cells, as generally found in striated muscles.

INTRODUCTION

Intracellular free Mg^{2+} is a cofactor of numerous enzymatic reactions and influences cellular functions through many different pathways (for review, see Flatman, 1984). Elucidation of its roles in the regulation of cellular functions under physiological and pathophysiological conditions requires an accurate measurement of the cytoplasmic free Mg^{2+} concentration ($[Mg^{2+}]_i$). $[Mg^{2+}]_i$ has been estimated with various methods, including ion-sensitive microelectrode (e.g., Blatter, 1990; Buri and McGuigan, 1990); nuclear magnetic resonance (NMR) (for review, see London, 1991); and optical indicators (e.g., Baylor et al., 1986; Raju et al., 1989). In skeletal and cardiac muscle cells, relatively large cells in which $[Mg^{2+}]_i$ has been studied most extensively, recent estimates of $[Mg^{2+}]_i$ appear to fall in the range of ~1 mM (e.g., Murphy et al., 1989; Blatter, 1990; Silverman et al., 1994). However, $[Mg^{2+}]_i$ of small cells, such as smooth muscle or nonmuscle cells, has been estimated to be 0.2–0.6 mM (e.g., Levy et al., 1988; Zhang et al., 1992; Nakayama et al., 1994). Kushmerick et al. (1986) measured $[Mg^{2+}]_i$ of smooth, cardiac, and skeletal muscles using ^{31}P-NMR, and reported that the basal $[Mg^{2+}]_i$ level in smooth muscles is approximately one-third of that in striated muscles. On the other hand, very similar $[Mg^{2+}]_i$ levels in smooth and skeletal muscles have been also reported (Ng et al., 1992). Technical difficulties in the quantification of $[Mg^{2+}]_i$ as well as animal species and tissue differences, probably underlie the inconsistency.

Fluorescent Mg^{2+} indicators have the advantage that fluorescence signals can be readily detected from small cells with a reasonable signal-to-noise ratio. Among the indicators, the "ratiometric" indicators, such as furaptra (also called mag-fura-2; Raju et al., 1989) and mag-indo-1, have been widely used to monitor the changes in $[Mg^{2+}]_i$ (Raju et al., 1989; Ishijima et al., 1991; Hurley et al., 1992; Westerblad and Allen, 1992; Zhang et al., 1992; Hongo et al., 1994; Silverman et al., 1994; Handy et al., 1996). Unfortunately, most of the above studies relied on the calibration of the indicators' fluorescence signals in solutions with simple salt compositions (in vitro calibration). Since the indicator properties (affinity and/or fluorescence) are likely altered in the intracellular environment, probably as a consequence of binding to proteins (e.g., Konishi et al., 1988; Kurebayashi et al., 1993), the validity of the estimated $[Mg^{2+}]_i$ values with the in vitro calibration remains uncertain. Two attempts to assess calibration parameters of Mg^{2+} indicators in the cell interior (intracellular calibration) have been reported in striated muscles, for furaptra in mouse skeletal muscle fibers (Westerblad and Allen, 1992), and for mag-indo-1 in rat ventricular myocytes (Silverman et al., 1994). However, there have been no reports, to our knowledge, regarding the intracellular calibration in other cell types whose cytoplasmic environments could differ from those of striated muscles.

This paper describes intracellular calibration of furaptra in smooth muscle cells of guinea pig tenia cecum. We have used 4-bromo-A23187, a divalent cation ionophore (Deber et al., 1985), as well as other ionophores to equilibrate $[Mg^{2+}]$ across the cell membrane. The method was analogous to that often used for the intracellular calibration of

Received for publication 2 June 1997 and in final form 3 September 1997.
Address reprint requests to Dr. Michiko Tashiro, Department of Physiology, The Jikei University School of Medicine, 3-25-8 Nishishinbashi, Minato-ku, Tokyo 105, Japan. Tel.: +81-3-3433-1279; Fax: +81-3-3433-1279; E-mail: tashiro@jikei.ac.jp.

0006-3495/97/12/3358/13 $2.00

Ca^{2+} indicators, but a much longer incubation time was necessary to reach quasi-steady levels of $[Mg^{2+}]_i$. From the intracellular calibration curve, basal $[Mg^{2+}]_i$ in guinea pig tenia cecum appears to be ~1 mM, which is similar to that generally reported for skeletal and cardiac muscle cells.

Some of the preliminary results of this study have been presented in abstract form (Tashiro et al., 1996a, b; 1997).

METHODS

Guinea pig tenia cecum

Guinea pigs (Hartley, male, 200–300 g) were sacrificed by cervical bleeding under deep anesthesia with ethyl ether, and longitudinal muscle strips (~200 μm wide, ~100 μm thick, and ~10 mm long) were dissected from tenia cecum at room temperature (22–25°C) under a binocular. The strip was slightly stretched to ~1.2 times of the slack length with one end attached to a force transducer (Bg-10, Kulite Semiconductor Products, Inc., Ridgefield, NJ). Fluorescence measurements were carried out in an experimental chamber on the stage of an inverted microscope (Diaphot, Nikon, Tokyo, Japan) equipped with a dual wavelength fluorometer (CAM 230, JASCO, Tokyo, Japan). The strip was initially perfused with normal Tyrode's solution containing (mM): 137.9 NaCl; 5.9 $KHCO_3$; 2.4 $CaCl_2$; 1.2 $MgCl_2$; 11.8 glucose; 5 HEPES; pH adjusted to 7.4 by NaOH at 25°C.

Experimental apparatus

The details of the optical apparatus have been described elsewhere (Konishi et al., 1993). In most experiments, two light beams of different wavelengths from two monochromators were switched at 100 Hz, and focused on a 900 μm length of the muscle strip with a 20× objective (CF Fluor 20, Nikon). The sample-and-hold output of the emitted fluorescence at 500 nm (±20 nm) for each excitation wavelength was low-pass filtered at 10 Hz and digitized at 20 Hz. For the measurement of the excitation spectrum, the excitation wavelength of a single light beam was sequentially changed from 330 nm to 420 nm with 5–10-nm steps. The UV exposure was limited by use of a pulse-controlled shutter opened only when the fluorescence was measured. The fluorescence signals were averaged over a 2-s period.

Solutions and chemicals

Ca^{2+}-free Tyrode's solution was prepared by substitution of 2.4 mM $CaCl_2$ of the normal Tyrode's solution with 0.1 mM EGTA. Solution with various Mg^{2+} concentrations ($[Mg^{2+}]$, 0–49 mM) for calibration contained (mM): 140–0 KCl; 10–0 NaCl; 0–50 $MgCl_2$; 1 EGTA; 10 PIPES; and pH 7.1. The KCl and NaCl concentrations were proportionally adjusted to keep ionic strength constant at 0.17 M. Free Mg^{2+} concentration was calculated under the assumption that the apparent dissociation constant for the Mg^{2+}-EGTA reaction was 16.9 mM at pH 7.1 and 25°C (Martell and Smith, 1974). The correction for Mg^{2+} chelated by EGTA was at most 5.6% of total Mg^{2+}. Bromo-A23187 (a divalent cation ionophore), monensin (Na^+ ionophore), and nigericin (K^+, H^+ ionophore) were added to the calibration solutions with 0.4–0.8% DMSO as a solvent. Furaptra (mag-fura-2, tetra potassium salt, lot 2211), furaptra-AM (mag-fura-2-AM, lot 2951), Br-A23187 (lot 2411), BAPTA-AM, and TPEN were purchased from Molecular Probes, Inc. (Eugene, OR). Monensin and nigericin were obtained from Sigma Chemical Co. (St. Louis, MO). Saponin (E. Merck, Darmstadt, Germany), Triton X-100 (Nacalai Tesque Inc., Kyoto, Japan), and caffeine (Nacalai Tesque Inc.) were used. All other chemicals were reagent grade.

In vitro fluorescence measurements

In vitro measurements were made in thin-walled quartz capillary tubes (i.d. 150 μm; Vitro Dynamics Inc., Rockaway, NJ) filled with calibration solutions containing 50 μM furaptra, and placed in the experimental chamber. Mg^{2+} binding caused blue-shift of the furaptra excitation spectrum with an isosbestic wavelength at 350 nm (see Fig. 5, *A* and *C*). In most of the following experiments, we therefore analyzed the ratio of fluorescence intensities excited at 382 nm [F(382)] and 350 nm [F(350)], as a Mg^{2+}-related signal [R = F(382)/F(350)], independent of the indicator concentration. The stability of the optical instruments was occasionally checked during the course of the study, by measuring furaptra R in the Mg^{2+}-free calibration solution as a standard; all measured values of R were normalized to the standard R value measured with the identical optical arrangement. The R value decreased from 1.0 to 0.08 upon Mg^{2+} binding, while the F(350) was independent of Mg^{2+} and proportional to the furaptra concentration.

From the values of furaptra R measured in the calibration solutions at 25°C with various $[Mg^{2+}]$ (small *filled circles* in Fig. 6), the dissociation constant for Mg^{2+} (K_D) was estimated to be 3.73 mM, which was close to that reported at near room temperature (3.6 mM at 23°C, Konishi and Berlin, 1993; 3.8 mM at 22°C, Westerblad and Allen, 1992). Addition of the ionophores in the calibration solutions did not appreciably change the R values (*crosses* in Fig. 6). It has been reported that either fluorescence or Mg^{2+} binding of furaptra is little affected by pH change between 6.5 and 7.2 (Konishi et al., 1993).

In vivo measurements

Only muscle strips that showed active spontaneous contractions were used for the experiments. After the background fluorescence was measured in the normal Tyrode's solution from the muscle strip in the absence of the indicator, the preparation was loaded with furaptra by incubation with the acetoxymethyl ester form of the indicator (4 μM furaptra-AM with 0.4% DMSO) for 30–40 min at room temperature. Furaptra-AM was then washed by continuous flow of the normal Tyrode's solution for at least 30 min before the first fluorescence measurement. After several measurements of F(350) and F(382) in the normal Tyrode's solution, the superfusing solution was switched to the Ca^{2+}-free Tyrode's solution for 40–60 min. The preparation was then incubated in the calibration solution, which contained Br-A23187, monensin, and nigericin to equilibrate primary cations (Mg^{2+}, Na^+, K^+, and H^+) on both sides of the cell membrane. Monensin and nigericin were included to eliminate the membrane potential. A relatively high concentration of each ionophore (20 μM each) was applied for the initial 30–50 min. This concentration of Br-A23187 was chosen after several trial and error experiments; concentrations higher than 20 μM caused substantial loss of the indicator. The ionophore concentrations were then reduced (10 μM Br-A23187, 5 μM monensin, 5 μM nigericin) and were maintained throughout the experiment. Some preparations were re-treated with high concentrations of ionophores (20 μM) in the later period of the experiments to ensure effective permeabilization of the cell membrane (e.g., Fig. 3 *B*), but the results were not significantly different from those obtained with the standard procedure. $[Ca^{2+}]$ in the calibration solution was kept low by 1 mM EGTA throughout the calibration run. This was important, because furaptra also binds Ca^{2+} and exhibits a fluorescence change indistinguishably different from that caused by Mg^{2+} (Raju et al., 1989). The bath solution was occasionally exchanged with a fresh solution, and the temperature was monitored with a thermister thermometer and maintained at 25 ± 1°C. The relatively low temperature was desirable to minimize leakage of the indicator; we found that the indicator fluorescence quickly declined at a temperature of 30°C or higher, which made the long-term fluorescence measurement extremely difficult. The indicator-related fluorescence was calculated by subtraction of the background fluorescence from the total fluorescence intensity measured in the same portion of the preparation. The change in the background fluorescence as a result of the ionophore treatment was taken into account and was corrected, as described in Results. For the measurement of excitation spectrum, F(350) was measured four times during the run to correct for the slow leakage of the indicator (for details, see Fig. 4 of Konishi et al., 1993).

Calibration of fluorescence signals

In order to calibrate furaptra R in terms of $[Mg^{2+}]$, estimates of three calibration parameters are required; R_{min}, R_{max}, and K_D. R_{min} and R_{max} are the R values at 0 $[Mg^{2+}]$ and saturating $[Mg^{2+}]$, respectively. The measured R values were least-squares-fitted to the theoretical binding curve (below) with the software, Deltagraph (Deltapoint, Inc., Monterey, CA); R_{min}, R_{max}, and K_D were taken to be adjustable variables. Using the estimates of these values for the intracellular indicator, $[Mg^{2+}]_i$ can be calculated based on the fluorescence ratio R measured in the cytoplasm by an equation for 1:1 binding:

$$[Mg^{2+}]_i = K_D(R - R_{min})/(R_{max} - R) \quad (1)$$

Determination of tissue ATP content

The amount of adenosine triphosphate (ATP) in the tissue was measured by the method first described by Strehler and McElroy (1957), which was successfully applied to tenia cecum tissue by Kishimoto et al. (1982). The small preparations (~2 mm wide, ~200 μm thick, and ~20 mm long) of longitudinal strips (wet weight, 2.4 ± 0.2 mg, n = 18) were exposed to either the normal Tyrode's solution or the calibration solution containing the ionophores for 3–13 h. The ionophore concentrations were high for the initial 40 min (20 μM Br-A23187, 20 μM monensin, and 20 μM nigericin), and were reduced to 10 μM Br-A23187, 5 μM monensin, and 5 μM nigericin for the rest of the period. The samples were then placed in 2 ml of boiling water for 5 min to extract ATP. The extract was immediately cooled to 0°C. The amount of ATP in the extract was measured by a photometer (Lumicounter 1000, Nichion, Chiba, Japan) with a highly purified luciferin-luciferase reagent (Lumit, Lumac, Landgraaf, Netherlands). The ATP content in the strips was calculated as mmol/kg wet weight.

A7r5 cells and cardiac myocytes

A7r5 cells from a smooth muscle cell line derived from the thoracic aorta of DBIX rat (American Type Culture Collection, Rockville, MD) were cultured in Dulbecco's modified Eagle's medium containing 10% fetal bovine serum. The cells, which were subcultured onto the thin glass attached to the bottom of the dishes, were used at the 3rd to 5th passage. After measurement of the background fluorescence from clusters of 5–10 cells in the normal Tyrode's solution, the cells were incubated with 2 μM furaptra-AM (0.2% DMSO) for 20 min at room temperature. Acetoxymethyl ester of the indicator was then washed with continuous flow of the normal Tyrode's solution for at least 10 min, and the fluorescence measurements were carried out from the cell clusters in the normal Tyrode's solution and Ca^{2+}-free Tyrode's solution at 25°C. In some experiments, the cells were further treated with the ionophores (20 μM Br-A23187, 20 μM monensin, 20 μM nigericin) in the calibration solutions.

Single ventricular myocytes were enzymatically isolated from rat hearts as previously described (Hongo et al., 1994). Isolated myocytes were superfused with the normal Tyrode's solution at 25°C in an experimental chamber, and then loaded with furaptra by incubation with 4 μM furaptra-AM for 20 min. Only rod-shaped cells that showed twitch responses to suprathreshold field stimulation were used for the following experiments with the protocol identical to that described above for A7r5 cells.

The same optical apparatus as described above for tenia cecum was used for the fluorescence measurements of A7r5 cells and cardiac myocytes with slight modifications; a 40× objective (CF Fluor 40, Nikon) was used to focus excitation light beams on optical field with ~150 μm diameter set by an aperture diaphragm. The background fluorescence measured before furaptra loading from individual cells (or cell clusters, in the case of A7r5 cells) was subtracted from the total fluorescence to calculate F(382), F(350), and R.

Statistical values

Statistical values are given as mean ± SE.

RESULTS

Localization of furaptra fluorescence

In general, ion indicator molecules loaded with their AM ester forms can be trapped inside intracellular organelles (compartmentalization). In the case of furaptra loaded in rat ventricular myocytes, ~16% of furaptra fluorescence appears to be compartmentalized from the cytoplasm (Hongo et al., 1994). To estimate the localization of furaptra in guinea pig tenia cecum, we applied saponin (50 μg/ml) to the preparations loaded with furaptra by our standard procedure (4 μM furaptra-AM, 40 min) (Fig. 1). Saponin, at this concentration, has been reported to permeabilize the cell membrane of smooth muscles without causing detectable changes in the sarcoplasmic reticulum and mitochondria (Somlyo et al., 1982; Yamamoto and van Breemen, 1986).

In four furaptra-loaded preparations, saponin treatment for 40 min reduced the F(350) to 11.4 ± 1.2% (n = 4). The residual fluorescence was entirely eliminated by the further application of Triton X-100 (1% v/v) for 20 min (Fig. 1). Because Triton X-100 was thought to solubilize the membranes of all organelles, this result suggests that most (~89%) of furaptra fluorescence was localized in the cytoplasm, with the small remaining fraction (~11%) localized in intracellular organelles. It is thus possible to measure Mg^{2+} concentration in the cytoplasm with furaptra. There is a possibility, however, that 11% of the fluorescence from the compartments influences the $[Mg^{2+}]_i$ measurement, if the local environment in the compartments is very different from that in the cytoplasm (see below).

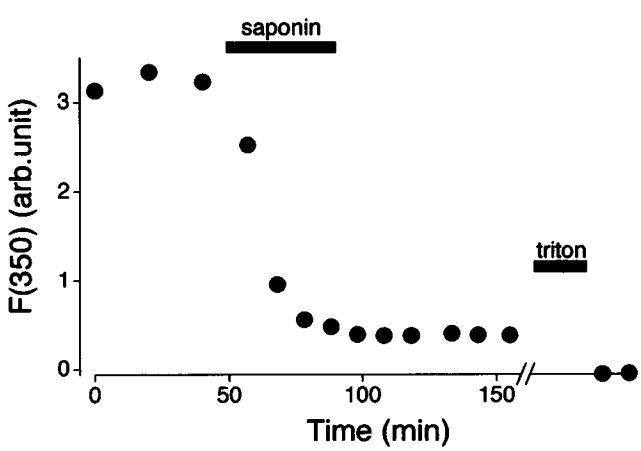

FIGURE 1 The effects of saponin and Triton X-100 on the furaptra fluorescence from the preparation. The background-subtracted F(350) values were plotted as a function of time (●). The preparation was initially incubated in the Ca^{2+}-free Tyrode's solution, and saponin (50 μg/ml) or Triton X-100 (1% v/v) was applied to the relaxing solution for the period indicated by the black bars. The composition of the relaxing solution was 71.5 mM K-methansulfonate, 5.1 mM Mg-methansulfonate, 4.3 mM Na_2ATP, 10 mM EGTA, and 10 mM PIPES (pH 7.1).

Alteration of the background fluorescence by the ionophores

The background fluorescence measured from preparations without furaptra loading was stable over several hours in the Ca^{2+}-free Tyrode's solution. However, we found that the background fluorescence was significantly altered by the treatment with Br-A23187. Fig. 2 shows an example of the experiments in which the background fluorescence was measured, as a function of time, during the ionophore treatment with the same protocol as that for the indicator-loaded preparations. The background fluorescence excited at either 382 nm or 350 nm increased linearly with time after the application of the ionophores. This increase was not observed when Br-A23187 was excluded from the calibration solution. The rates of the change of the background fluorescence, relative to the levels before the ionophore treatment, were 31.2 ± 5.2%/h and 6.9 ± 2.4%/h (n = 4) at 382 nm and 350 nm excitation, respectively, in the calibration solution with 0 mM [Mg^{2+}]. The increased background fluorescence was largely reversed by cell lysis with Triton X-100 (Fig. 2); in four preparations treated with the ionophores for 5 h, the application of Triton X-100 (1% v/v) for 20 min decreased the background fluorescence by 48.0 ± 5.4% at 382 nm and by 37.2 ± 4.7% at 350 nm excitation.

Because it was not possible to measure the background fluorescence from the furaptra-loaded preparations, a somewhat indirect estimation was used. At the end of each calibration run, the preparation was treated with 1% v/v Triton X-100 to dissipate all of the indicator fluorescence (cf. Fig. 1). From the background fluorescence intensity measured in the lysed preparation, the background fluorescence at the end of the run was calculated by using the average reduction of the background fluorescence by Triton (i.e., 48% and 37% for 382-nm and 350-nm excitation, respectively). The background fluorescence at any time during the calibration run was then estimated, for each excitation wavelength, assuming a linear increase in the background fluorescence with treatment time (cf. *solid lines* in Fig. 2). In seven furaptra-loaded preparations treated with the ionophores for 3 to 8 h, the average rates of increase in the background fluorescence (relative to the initial levels) estimated using this method were 37.4 ± 6.3%/h for 382-nm and 9.4 ± 1.7%/h for 350-nm excitation. These values are in reasonably good agreement with those measured in the preparations that were not loaded with furaptra (above).

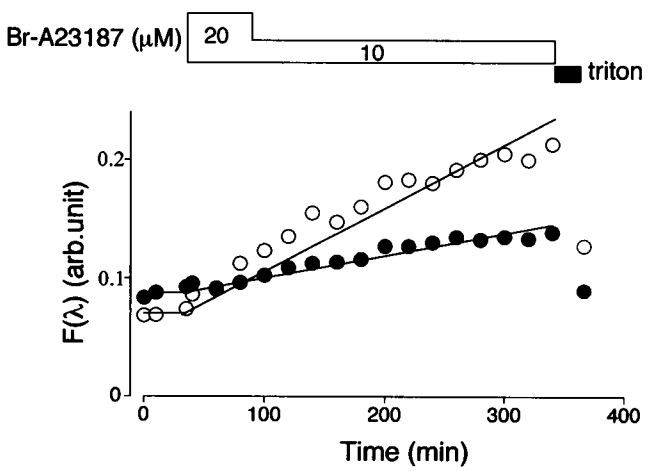

FIGURE 2 Long-term observation of the background fluorescence excited at 350 nm (●) and 382 nm (○) from the preparation treated with the ionophores. Br-A23187 (20-10 μM), monensin (20-5 μM), and nigericin (20-5 μM) were added to the calibration solution containing 0 mM [Mg^{2+}] for the period indicated above (for simplicity, only Br-A23187 concentration was shown). For each wavelength, the mean level of the fluorescence in the absence of the ionophores, and the least-squares-fitted line for data points in the presence of the ionophores are shown. At the end of the experiment, 1% (v/v) Triton X-100 was applied as indicated by the black bar.

The increase of background fluorescence seemed to be slowed (or "saturated") with the longer incubation with ionophores. In two furaptra-loaded preparations treated with the ionophores for 16 to 17 h, the estimated increment of the background fluorescence was, on average, 200% and 58% at 382 nm and 350 nm, respectively. These values are much smaller than those expected from the linear increase with time. For the early fluorescence measurements (treatment time <7 h) of these runs, we therefore calculated the background level using the average rates of increase obtained from the above seven runs (i.e., 37.4%/h for 382 nm and 9.4%/h for 350 nm).

The measurements of the background fluorescence described above (and shown in Fig. 2) were carried out in the Mg^{2+}-free calibration solution. However, the ionophore-induced increase in the background fluorescence might also be influenced slightly by the levels of [Mg^{2+}] in the calibration solution. In one experiment with no indicator loading, a preparation was incubated in the calibration solution containing 0 mM [Mg^{2+}] for ~4 h, during which the rise of the background fluorescence was monitored. The [Mg^{2+}] in the bathing solution was then changed to 49 mM, and the background fluorescence was measured 20 and 40 min later. The solution [Mg^{2+}] was then returned back to 0 mM. The bracketed measurements at 0 mM [Mg^{2+}] were linearly interpolated to form the baseline. The background values measured at 49 mM [Mg^{2+}] were 30% (mean of 30% and 29%) and 17% (mean of 18% and 16%) higher at 382 nm and 350 nm, respectively, than the baseline values for 0 mM [Mg^{2+}]. In another experiment with a very similar protocol, the background fluorescence levels were elevated at 4 mM [Mg^{2+}] by 15% (mean of 22% and 8%) and 8% (mean of 12% and 4%) at 382 nm and 350 nm, respectively. No detectable change in the background fluorescence was observed at 1 mM [Mg^{2+}] in the other preparation.

Based on the above observations, the final estimates of the background fluorescence included correction for the small additional increase at [Mg^{2+}] > 1 mM with the factors estimated above at 4 mM and 49 mM [Mg^{2+}]; correction factors for 2 mM and 8 mM [Mg^{2+}] were somewhat arbitrarily taken to be proportional between two adjacent [Mg^{2+}] values. This final correction of the background

fluorescence, however, only slightly influenced the resultant intracellular calibration curve (see Discussion).

Since the background fluorescence was only a minor fraction of the total fluorescence intensity measured after the indicator loading (~2% at 382 nm and ~5% at 350 nm excitation), a small change in the background fluorescence should not influence the results of analysis at the beginning of the calibration run. The correction of the background fluorescence could not be ignored toward the end of the run, because of the gradual decrease of the indicator fluorescence (below) and the increase in the background fluorescence. The changes of R after background correction were generally within ± 0.02 (-0.066 at the maximum). We did not further investigate the source of the ionophore-induced change in the background fluorescence.

Measurements of the indicator fluorescence

Fig. 3 shows examples of the calibration runs in which the Mg^{2+}-independent F(350) and the Mg^{2+}-dependent R [F(382)/F(350)] were followed for ~8 h. The slow decrease in the F(350) probably reflected the leak of the indicator from the cell interior, and during the first 90 min did not accompany any significant change in R. Removal of extracellular Ca^{2+} (*arrows* in Fig. 3) generally caused little change in R (ΔR within $\pm$ 0.01, 12 of 19 preparations). However, we occasionally observed a small (but non-negligible) change in the R when the preparations were transferred to the Ca^{2+}-free solution (e.g., Fig. 3 *A*, ~30 min after the downward arrow). The small increase in R, as seen in Fig. 3 *A*, could be explained by the lowering of $[Ca^{2+}]_i$ in damaged cells in the preparations, if a substantial population of cells was damaged during the preparation process, resulting in a very high $[Ca^{2+}]_i$ in the normal Tyrode's solution. For the purpose of basal $[Mg^{2+}]_i$ estimation, we therefore did not use R values that were influenced by the removal of extracellular Ca^{2+}. The R was very stable for many hours in the Ca^{2+}-free Tyrode's solution (e.g., see Fig. 3 *A* of Tashiro and Konishi, 1997). The long-term stability of R suggests that incompletely hydrolyzed AM esters, if any, did not affect the fluorescence measurement in the present study.

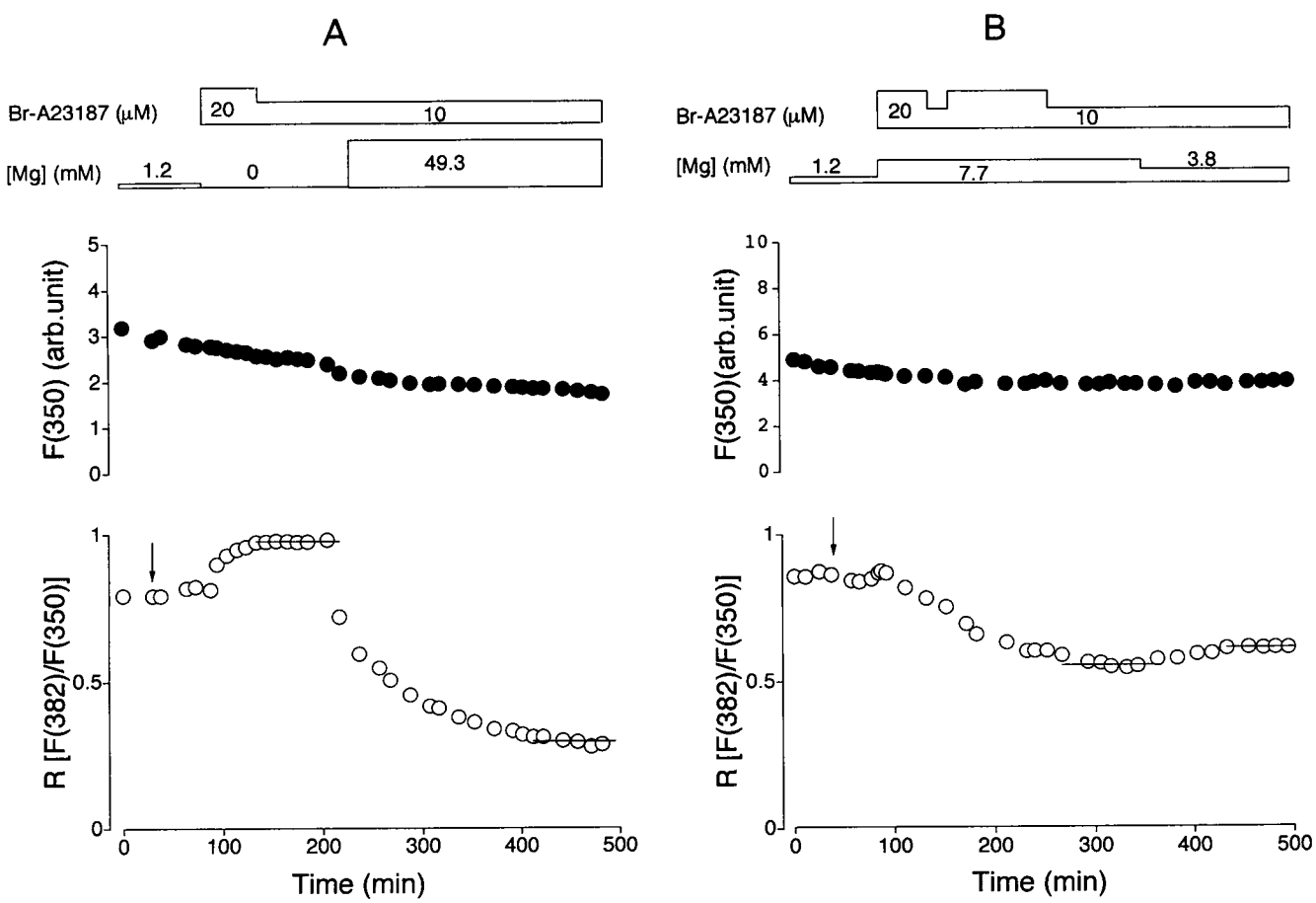

FIGURE 3 The change in the fluorescence ratio R at various $[Mg^{2+}]_o$ after treatment with ionophores. (*A*) and (*B*) are examples of two separate experiments in which furaptra F(350) (●, *upper panel*) and the ratio R (○, *lower panel*) were plotted as a function of time. In (*A*) and (*B*) normal Tyrode's solution was substituted with Ca^{2+}-free Tyrode's solution at the time indicated by arrows, and the ionophores were added to the calibration solution with various $[Mg^{2+}]$ indicated above. The ionophore solutions contained either 20 μM Br-A23187 (plus 20 μM monensin and 20 μM nigericin), or 10 μM Br-A23187 (plus 5 μM monensin and 5 μM nigericin); the Br-A23187 concentration is indicated at the top.

Application of the ionophores caused no appreciable changes in the F(350), but did cause two clear changes in *R:* a) a small increase with rapid onset (within 5 min), as clearly seen in Fig. 3 *A*, and b) the slow change that follows the rapid increase. We called the initial rapid component a) ΔR_{jump}; the details of the properties of the ΔR_{jump} component will be described in the next section. The slow component b), ΔR_{slow}, was either upward or downward depending on $[Mg^{2+}]$ in the calibration solutions. *R* increased at low $[Mg^{2+}]_o$ (e.g., 0 mM; Fig. 3 *A*), decreased at high $[Mg^{2+}]_o$ (e.g., 7.7 mM; Fig. 3 *B*), and was essentially unchanged at ~1 mM $[Mg^{2+}]_o$ (not shown). The direction of the ΔR_{slow} was consistent with Mg^{2+} movement down the concentration gradient across the permeabilized cell membrane with Br-A23187. The ΔR_{slow} was analyzed as a $[Mg^{2+}]_i$-related signal in the following sections.

R reached an apparently steady level in 2–5 h at constant $[Mg^{2+}]_o$. When $[Mg^{2+}]_o$ was set to a new level, *R* slowly changed again to reach a new quasi-steady level (Fig. 3, *A* and *B*). It generally took longer to reach the steady level at very high $[Mg^{2+}]_o$ (e.g., 49 mM; Fig. 3 *A*). We therefore carried out experiments of prolonged time base, in which two preparations were incubated in the calibration solution with 49 mM $[Mg^{2+}]$ for ~10 h and ~14 h (not shown). The quasi-steady level of *R* from these preparations were 0.26 and 0.29. These values were very similar to those estimated after 5 h of incubation (0.28, see Fig. 3 *A*).

Properties of the ΔR_{jump}

The small ΔR_{jump} component of *R* (Fig. 3) was always a positive change and consistently observed in all experiments with the ionophores. The peak size of the ΔR_{jump} was 0.049 ± 0.004 (n = 3), when measured 5–10 min after application of the calibration solution containing 1 mM Mg^{2+} and the ionophores. Because a ΔR_{jump} of a very similar size (0.055 ± 0.004, n = 3) was observed in the calibration solution containing only 20 μM Br-A23187, the ΔR_{jump} was probably induced by Br-A23187. Application of the calibration solution without the ionophores caused no significant change in *R* (0.0098 ± 0.0043, n = 3).

Because the wavelength-dependence of the ΔR_{jump} was consistent with a Mg^{2+}- (or Ca^{2+}-) dependent fluorescence change (see the next section), ΔR_{jump} was thought to reflect the decrease of Mg^{2+} (or Ca^{2+}) binding of the indicator, rather than some nonspecific artifact of the ionophore. Fig. 4 *A* shows examples of the ΔR_{jump} observed in various $[Mg^{2+}]_o$. Application of the ionophores (*arrows* in Fig. 4 *A*) consistently induced a small upward shift of *R* (or ΔR_{jump}) within 5–10 min, which was followed by a slow change in *R* (or ΔR_{slow}). In contrast to the clear $[Mg^{2+}]_o$-dependence of the ΔR_{slow} (see reversal of the direction, Fig. 4 *A*), the direction of the ΔR_{jump} was never reversed at $[Mg^{2+}]_o$ between 0 and 8 mM. Moreover, the size of the ΔR_{jump} (measured 5–10 min after the ionophore treatment) was not markedly dependent upon $[Mg^{2+}]_o$ between 1 and 8 mM

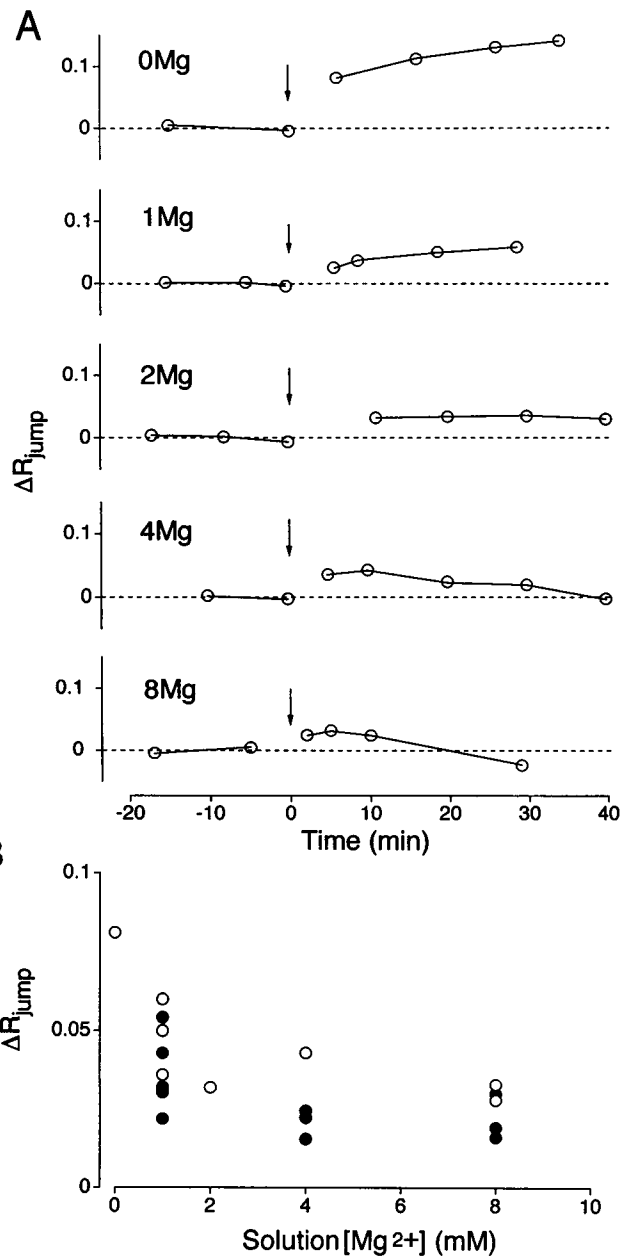

FIGURE 4 The rapid change in *R* (ΔR_{jump}) after the application of ionophores (20 μM Br-A23187, 20 μM monensin, and 20 μM nigericin), at various $[Mg^{2+}]_o$. (*A*) The change in *R* from the average value in Ca^{2+}-free Tyrode's solution was plotted as a function of time. The ionophores were applied at time zero on the abscissa (*arrows*), to the calibration solutions containing various $[Mg^{2+}]$ as indicated (mM). Panels represent examples from different preparations. (*B*) The relation between the size of the ΔR_{jump} measured at 5–10 min after the application of the ionophores (*ordinate*) and $[Mg^{2+}]$ in the calibration solution (*abscissa*). (○), data points obtained from eight different preparations of tenia cecum. (●), data from 11 clusters of A7r5 cells.

(*open circles* in Fig. 4 *B*). One large ΔR_{jump} observed at 0 mM $[Mg^{2+}]_o$ might have been influenced by the overlapping of ΔR_{slow} in the upward direction (*top trace* of Fig. 4 *A*). The finding that there was no reversal of the ΔR_{jump} even at 8 mM $[Mg^{2+}]_o$ led us to assume that the ΔR_{jump} was

related to the decrease of $[Mg^{2+}]$ (or $[Ca^{2+}]$) in some compartments other than the cytoplasm.

The most obvious candidate of such compartments is Ca^{2+} stores. Because 1) ~11% of the indicator fluorescence appeared to be compartmentalized, as described above; and 2) A23187 has been reported to permeabilize the membranes of the Ca^{2+} stores more effectively than the cell membrane (Itoh et al., 1985), it is possible that the ionophore rapidly permeabilizes the Ca^{2+} stores, leading to the depletion of Ca^{2+}, and consequently generates ΔR_{jump}. To test this hypothesis, the ΔR_{jump} was measured (at 1 mM $[Mg^{2+}]_o$) in the preparations depleted of Ca^{2+} using two different procedures: 1) the preparations were pretreated with 20 mM caffeine plus a low concentration of Br-A23187 in the Ca^{2+}-free Tyrode's solution. In three preparations pretreated with 0.2 μM, 1 μM, and 2 μM Br-A23187, the size of the ΔR_{jump} was 0.041, 0.028, and 0.020, respectively. 2) In two preparations loaded with a Ca^{2+} chelater BAPTA (20 μM BAPTA-AM, for 80–120 min), the average amplitude of the ΔR_{jump} was 0.032. The combination of BAPTA loading and 20 mM caffeine reduced the ΔR_{jump} to 0.012 in one preparation. Thus, the depletion of Ca^{2+} stores by the ionophore might be partially responsible for the generation of the ΔR_{jump} component, but the results were not conclusive. Contribution of intracellular heavy metals (e.g., Zn^{2+}, etc.), if any, appears to be minor; in one preparation loaded with TPEN (50 μM), a heavy metal chelater, ΔR_{jump} with a moderate size (0.034), was observed at 1 mM $[Mg^{2+}]_o$.

An alternative possible mechanism involved in the generation of the ΔR_{jump} is a change in local environment, which lowers Mg^{2+} (or Ca^{2+}) affinity of a subpopulation of furaptra, even without changes in local $[Mg^{2+}]$ (or $[Ca^{2+}]$). Although we could not conclusively characterize the mechanism, the ΔR_{jump} was considered to be a signal unrelated to $[Mg^{2+}]_i$. For the analysis of $[Mg^{2+}]_i$, we therefore decided to add the offset value of the ΔR_{jump} to R values measured from intact preparations, before Eq. 1 was applied (see sample calculation in Results). For this purpose, we used the mean amplitude of the ΔR_{jump} at 1 mM $[Mg^{2+}]_o$, 0.05 (n = 6), as the ΔR_{jump} was thought to be least influenced by the overlap of the ΔR_{slow} at 1 mM $[Mg^{2+}]_o$.

Spectra of the fluorescence change

To determine whether the change in R shown in Fig. 3 was caused by Mg^{2+} binding (association or dissociation) of the indicator, rather than by artifacts of some kind unrelated to Mg^{2+}, the fluorescence excitation spectra of furaptra (330–420 nm, 10-nm steps) were measured from the preparations (Fig. 5). After the measurement of the spectrum in the Ca^{2+}-free Tyrode's solution (*crosses* in *A* and *C*), the preparations were treated with the ionophores, and the spectrum measurement was repeated at various $[Mg^{2+}]_o$. The increase in the background fluorescence during the ionophore treatment was estimated (and corrected) for each wavelength, as described above in connection with Fig. 2; the method was based on the residual fluorescence after Triton X-100 treatment and the average reduction of the background fluorescence by Triton X-100 measured, at each wavelength, in three preparations in the absence of furaptra (not shown).

The wavelength dependence of the intracellular fluorescence change, calculated by the subtraction of one spectrum from another, was very similar to the indicator's Mg^{2+} difference spectrum in salt solutions. The spectral shape of the ΔR_{jump} (*crosses* in Fig. 5 *B*) was also approximately matched to the in vitro Mg^{2+} difference spectrum. Thus, both the ΔR_{jump} and the ΔR_{slow} are consistent with the changes in Mg^{2+} (or Ca^{2+}) binding of furaptra.

Intracellular calibration curve

Under the assumption that $[Mg^{2+}]_i$ reached the same level as $[Mg^{2+}]_o$ at the quasi-steady state of the R, we could construct an intracellular calibration curve, by which $[Mg^{2+}]_i$ could be calculated from R measured in the preparations. Each open symbol in Fig. 6 represents the mean value of several measurements taken at a quasi-steady state (see Fig. 3). Eighteen data points were accumulated from 10 preparations, because only 1 to 3 quasi-steady levels could be achieved in a single preparation. The quasi-steady level of R for each pMg showed a good agreement with a reasonably small scatter among different preparations and different sequences of $[Mg^{2+}]$ change; the quasi-steady level was apparently independent of the direction of the change in $[Mg^{2+}]_o$ (and therefore $[Mg^{2+}]_i$), as best seen at pMg 3 and 2.4. The open symbols in Fig. 6 are best described by Eq. 1 with R_{min} 0.986, R_{max} 0.199, and K_D 5.43 mM. In comparison with the in vitro curve, the intracellular calibration curve gave larger K_D and R_{max} values by factors of 1.46 and 2.49, respectively, with very similar R_{min}.

ATP content

During the calibration runs described above, Mg^{2+} might have been actively extruded from the cells, utilizing cellular ATP, to counteract Mg^{2+} influx through the permeabilized cell membrane by Br-A23187. In the presence of such an active transport, Mg^{2+} on both sides of the cell membrane should reach apparent equilibrium at $[Mg^{2+}]_i$ lower than $[Mg^{2+}]_o$. To check this possibility, we measured ATP content in the preparations treated with the ionophores for different periods of time (Table 1).

Tissue ATP content of the preparations was ~1 mmol/kg wet weight, similar to earlier reports (Butler and Davies, 1980; Kishimoto et al., 1982), and was maintained essentially unchanged for 13 h in normal Tyrode's solution. The treatment with the ionophores added to the solution with 49 mM $[Mg^{2+}]_o$ markedly reduced the ATP content (to ~3%) within 8 h, and nearly completely depleted cellular ATP (<1%) within 13 h. The decrease in ATP might be due to the uncoupling of mitochondrial oxidative phosphorylation

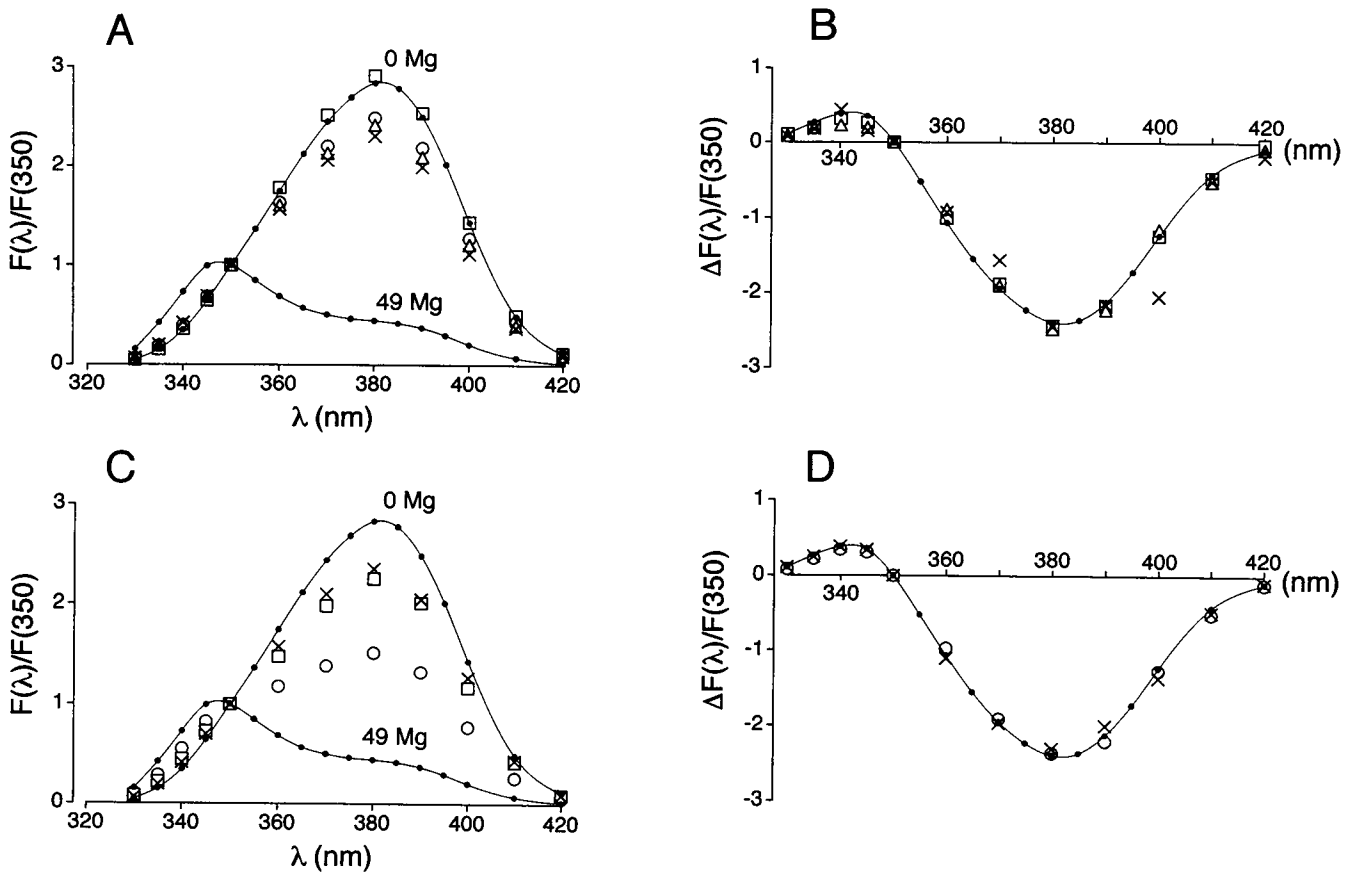

FIGURE 5 Fluorescence excitation spectra of furaptra measured in two different preparations [*open symbols* in (*A*) and (*C*)]. (*A*) Excitation spectra measured before the ionophore treatment in Ca^{2+}-free Tyrode's solution (×), 5–10 min after the treatment with the ionophores (20 μM Br-A23187, 20 μM monensin, and 20 μM nigericin) in the calibration solution with 1 mM $[Mg^{2+}]$ (△), and in the near steady-state at 1 mM $[Mg^{2+}]_o$ (○) and 0 mM $[Mg^{2+}]_o$ (□). Each spectrum has been normalized to F(350) to correct for the decrease in the indicator concentration. (*B*) The difference spectra obtained from the experiment shown in (*A*) by: (×), subtraction of △ from × in (*A*); (△), subtraction of □ from △ in (*A*); (□), subtraction of □ in (*A*) from spectrum measured in 2 mM $[Mg^{2+}]_o$ [not shown in (*A*)]. (*C*) Data from a similar experiment as shown in (*A*). The spectra were measured in the Ca^{2+}-free Tyrode's solution (×), and in the calibration solutions containing 2 mM $[Mg^{2+}]$ (□) and 8 mM $[Mg^{2+}]$ (○) in the presence of the ionophores. (*D*) The difference spectra calculated from data shown in (*C*) by: (×), subtraction of × from ○ in (*C*); (○), subtraction of □ from ○ in (*C*). Small filled circles in (*A*) and (*C*) are the in vitro spectra of ~50 μM furaptra in the calibration solutions of 0 mM $[Mg^{2+}]$ (0 Mg) and 49 mM $[Mg^{2+}]$ (49 Mg) placed in quartz capillaries. A solid line through data points was drawn by splice interpolation. The Mg^{2+} difference spectrum calculated by subtraction of the 0 Mg spectrum from the 49 Mg spectrum is shown in (*B*) and (*D*). In (*B*) and (*D*), each data set obtained in the preparations has been scaled to fit the in vitro difference spectrum.

by monensin and/or nigericin (Lardy et al., 1958; Kishimoto et al., 1982). It is thus very unlikely that an ATP-driven Mg^{2+} pump, even if present, significantly influenced the quasi-steady level at 49 mM $[Mg^{2+}]_o$, at least in two runs of the extended time scale (~10 h and ~14 h, see above). Because this experiment was only carried at one $[Mg^{2+}]$ level (49 mM), no information was available regarding a change in ATP content at other $[Mg^{2+}]$ levels.

Estimation of basal $[Mg^{2+}]_i$ in tenia cecum

With the intracellular calibration curve obtained in the ionophore-treated preparations (Fig. 6), the basal $[Mg^{2+}]_i$ of intact preparations was calculated. In 12 preparations which satisfied our criteria (little change in *R*, within ± 0.01, by removal of extracellular Ca^{2+}), the measured *R* value in normal Tyrode's solution was 0.816 ± 0.005. After the correction for the ΔR_{jump} (+0.05), the *R* value was 0.866 ± 0.005. The mean basal $[Mg^{2+}]_i$ thus calculated was 0.98 ± 0.05 mM (Table 2).

A7r5 cells and cardiac myocytes

Localization of furaptra in A7r5 cells was estimated with a protocol very similar to that shown in Fig. 1 for tenia cecum preparations (not shown). Furaptra F(350) from A7r5 cells was quickly reduced to 7.5 ± 1.2% (n = 8) after the application of saponin (50 μg/ml), suggesting that only a minor fraction of furaptra fluorescence was compartmentalized from the cytoplasm.

In clusters of 5 to 10 A7r5 cells, furaptra *R* could be reliably measured. Extracellular perfusion with the Ca^{2+}-free Tyrode's solution caused little change in *R* (within ± 0.01) in most experiments (33 of 35). After the application

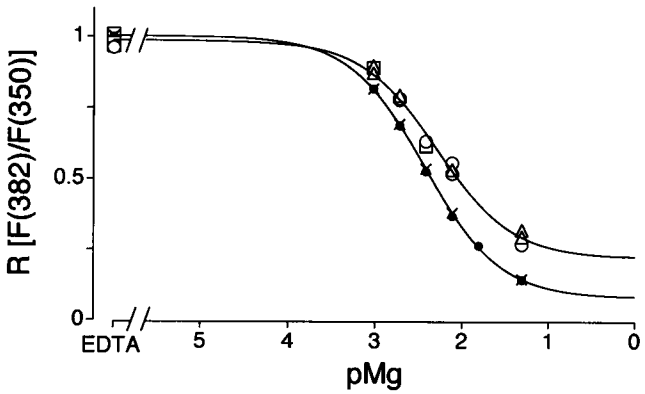

FIGURE 6 In vitro and intracellular calibration curves of furaptra. The quasi-steady levels of R obtained from the experiments of the type shown in Fig. 3 (*open symbols*) are plotted versus pMg ($-\log_{10}[Mg^{2+}]$). In each experiment, the preparation was transferred from the Ca^{2+}-free Tyrode's solution to the ionophore solution with a given $[Mg^{2+}]$ level (from 0 to 49 mM), and ○ were first obtained. In six experiments, the bath $[Mg^{2+}]$ was further changed, and additional data points were obtained in the new steady level; △ and □ were obtained by increasing and decreasing $[Mg^{2+}]$, respectively. Small filled circles and X's are the data obtained in vitro in the calibration solutions in the absence or in the presence of the ionophores (10 μM Br-A23187, 10 μM monensin, and 10 μM nigericin), respectively. Solid lines are theoretical 1:1 binding curves least-squares-fitted for data sets obtained in vitro (small filled circles and X's) and in the ionophore-treated preparations (○, △, and □). The best fitted values of K_D, R_{max}, and R_{min} are 3.72 mM, 0.080, and 1.008 for the in vitro curve, and 5.43 mM, 0.199, and 0.986, respectively, for the intracellular curve.

of the ionophores (Br-A23187, monensin, and nigericin; 20 μM each) to the calibration solution, R underwent changes similar to those seen in tenia cecum (cf. Fig. 3); The increase with the rapid onset (within 5 min), or ΔR_{jump}, was followed by the slow component, ΔR_{slow}. The ΔR_{jump} and ΔR_{slow} in A7r5 cells share many properties with those in tenia cecum. The amplitude of the ΔR_{jump} was not significantly influenced by $[Mg^{2+}]_o$ between 1 and 8 mM, as shown in Fig. 4 *B* (*filled circles*). The ΔR_{slow} was very slight at 1 mM $[Mg^{2+}]_o$, and was clearly downward (a decrease in R) at 8 mM $[Mg^{2+}]_o$ (not shown).

Because we did not follow R long enough to achieve the quasi-steady level in A7r5 cells, the relation between R and $[Mg^{2+}]_i$ could not be obtained. We therefore tentatively used the calibration curve obtained in tenia cecum preparations (Fig. 6) to estimate the basal $[Mg^{2+}]_i$ of this cell type.

TABLE 1 ATP content

Incubation Time	0	3 h	8 h	13 h
Control	1.08 ± 0.032	—	1.17 ± 0.070	1.06 (0.67, 1.45)
Ionophore-treated	—	1.05 ± 0.17	0.032 ± 0.016	0.0079 ± 0.0019

Values are given in mmol/kg wet weight. Values of ATP content are expressed as mean ± SE of 3–4 preparations, except for one entry where an average value and two raw values (parentheses) of two preparations are given. Dashed entries indicate that no measurement was made. A $[Mg^{2+}]_o$ of 49 mM was used for the ionophore-treated cells.

TABLE 2 Estimation of basal $[Mg^{2+}]_i$

		Estimated $[Mg^{2+}]_i$ (mM)	
	ΔR_{jump}	In vitro Calibration	Intracellular Calibration (with ΔR_{jump} Correction)
Tenia cecum	0.052 ± 0.005 (6)	0.95 ± 0.03 (12)	0.98 ± 0.05 (12)
A7r5 cells	0.035 ± 0.004 (6)	0.70 ± 0.01 (33)	0.74 ± 0.02 (33)
Cardiac myocytes	0.035 ± 0.006 (5)	0.95 ± 0.04 (9)	1.13 ± 0.06 (9)

Comparison of basal $[Mg^{2+}]_i$ in three different cell types. The ΔR_{jump} was measured in the calibration solution containing 1 mM Mg^{2+} (and 4 mM Mg^{2+} in the case of cardiac myocytes; see text). The values of $[Mg^{2+}]_i$ are mean ± SE from number of preparations in parentheses. The intracellular curve was applied after correction for the ΔR_{jump}.

In 33 cell clusters, the background-subtracted R value was 0.856 ± 0.002 in normal Tyrode's solution; this value was influenced little by extracellular Ca^{2+} (see above). After the correction of R measured in each experiment with an average amplitude of ΔR_{jump} of 0.035 (±0.004, n = 6) in 1 mM $[Mg^{2+}]_o$, the basal $[Mg^{2+}]_i$ was calculated to be 0.74 ± 0.02 mM (Table 2).

A very similar approach was applied to several ventricular myocytes isolated from rat hearts. R measured in 9 of 12 quiescent myocytes in normal Tyrode's solution was minimally changed (within ±0.01) by perfusion with the Ca^{2+}-free Tyrode's solution. The changes in R induced by the ionophores were qualitatively similar to those described above for tenia cecum and A7r5 cells, with a clear ΔR_{jump} 5–10 min after the application of the ionophores. The amplitude of the ΔR_{jump} was +0.052 at 1 mM $[Mg^{2+}]_o$ (1 myocyte) and +0.032 ± 0.007 at 4 mM $[Mg^{2+}]_o$ (4 myocytes). At 4 mM $[Mg^{2+}]_o$, a subsequent decrease in R was observed in the slow time course similar to that shown in Fig. 4 *A*. From the R values measured in normal Tyrode's solution, 0.816 ± 0.006 (n = 9), and the average size of ΔR_{jump}, +0.035 (average of five measurements at 1 mM or 4 mM $[Mg^{2+}]_o$), the basal $[Mg^{2+}]_i$ was estimated to be 1.13 ± 0.06 mM (Table 2).

DISCUSSION

Intracellular calibration of furaptra

We used ionophores to calibrate furaptra's fluorescence signals in terms of $[Mg^{2+}]_i$. The intracellular calibration of furaptra by the injection of a large amount of EDTA and/or $MgCl_2$ has been reported in mouse skeletal muscle fibers (Westerblad and Allen, 1992), but the application of this method to cells with smaller size seems to be technically difficult. The present calibration method is easily applicable to small cells, such as smooth muscle cells, in a relatively straightforward manner, if steps are taken to allow for some complications such as those unexpectedly incurred in the present study (see Results).

Bromo-A23187, a nonfluorescent divalent cation ionophore, has been widely used to equilibrate $[Ca^{2+}]$ across the

cell membrane for the calibration of Ca^{2+} indicators (e.g., Li et al., 1987; Williams and Fay, 1990). Attempts to use Br-A23187 (or other ionophores) to calibrate the signals of intracellular Mg^{2+} indicators have generally been unsuccessful (Raju et al., 1989; Ishijima et al., 1991; Westerblad and Allen, 1992), due to the slow change in $[Mg^{2+}]_i$ after ionophore treatment (see Fig. 3). The slow time course of the $[Mg^{2+}]_i$ change is probably due to the fact that, in comparison with Ca^{2+}, a much larger amount of Mg^{2+} must be transported to reach equilibrium, and because the Mg^{2+} transport rate of A23187 is several times lower than that for Ca^{2+} (Reed and Lardy, 1972). It is therefore critical to preserve the cell membrane structure for a long time without gross disruption, which causes a rapid loss of the indicator fluorescence. We relied on the long-term stability of muscle strips of guinea pig tenia cecum, which maintain the spontaneous activity, as well as tissue ATP content (Table 1), for many hours in normal Tyrode's solution.

Silverman et al. (1994) applied an analogous method to calibrate another ratiometric Mg^{2+} indicator mag-indo-1 in rat ventricular myocytes. They used 20 μM Br-A23187, in combination with valinomycin (a K^+ ionophore), nigericin, and a mitochondrial uncoupler, but the calibration process was not described in detail. In the present study, we also found two complications related to the use of the ionophores, which should be taken into account for the analysis of indicator fluorescence signals.

First, the background fluorescence in the Br-A23187-treated preparations increased with time. The time course of the background fluorescence change was approximately linear up to 5 h after the treatment with Br-A23187 at 0 mM $[Mg^{2+}]_o$ (Fig. 2), whereas R reached the steady level within 1–2 h, and did not change further (see Fig. 3 *A*). It is therefore unlikely that the change in $[Mg^{2+}]_i$ is primarily responsible for the background fluorescence change. We rather speculate that the binding of Br-A23187 to the cellular membranes might make the ionophore weakly fluorescent. The correction for this change in the background fluorescence was relatively minor in the present study, although not negligible, and was reasonably straightforward because of its approximate linearity with time (Fig. 2). Although additional correction was made for the observed increase in the background fluorescence at $[Mg^{2+}] > 1$ mM in the bathing solution (see Results), similar estimates of the calibration parameters are obtained even without this correction; R_{min}, R_{max}, and K_D values are 0.987, 0.222, and 5.13 mM. Calculated values of $[Mg^{2+}]_i$ with or without the additional correction differ only by <1.5% for $[Mg^{2+}]$ in the range between 0.2 mM and 7 mM.

Second, more puzzling was the ΔR_{jump} component noted shortly after the application of Br-A23187. Although a part of the ΔR_{jump} could be attributed to the permeabilization of the subcellular membranes by Br-A23187, we could not fully identify the origin of this component. A qualitatively similar ΔR_{jump} was observed in A7r5 cells and cardiac myocytes, but the underlying mechanism of ΔR_{jump} in these and in tenia cecum preparations might not necessarily be the same. The existence, properties, and amplitude of the ΔR_{jump} component should be analyzed for individual preparations, indicators, and experimental conditions.

Alterations of the properties of furaptra by the intracellular environment

It has been reported that indicator properties are likely altered in the intracellular environment, because of indicator binding to cellular constituents (e.g., Konishi et al., 1988; Kurebayashi et al., 1993). In the present study, among three calibration parameters, R_{max} and K_D values estimated in the ionophore-treated preparations were larger than the parameters in solutions by factors of 2.49 and 1.46, respectively, while R_{min} was only slightly decreased in the cytoplasm. The present results may be compared with those reported by Westerblad and Allen (1992), who injected a high concentration of $MgCl_2$ and/or EDTA into mouse skeletal muscle fibers to calibrate the intracellular furaptra fluorescence ratio signal [R = F(340)/F(360)]. They found that, in the cytoplasm, R_{min}, R_{max}, and S_{F2}/S_{b2} [the ratio of F(360) of Mg^{2+}-free and Mg^{2+}-bound indicator] were essentially unchanged, and K_D was slightly increased (21%). The most obvious difference between the present results and those by Westerblad and Allen (1992) seems to lie in the alteration of R_{max} in the intracellular environment.

One possible explanation for this difference might be that the intracellular increase in R_{max} found in the present study is due to incomplete equilibration of $[Mg^{2+}]$ across the cell membrane, particularly at very high $[Mg^{2+}]_o$. This could happen, if Mg^{2+} is actively pumped out of the cell to counterbalance Mg^{2+} influx. Although we cannot completely rule it out, we think that this possibility is unlikely for the following reasons: 1) Na^+ concentration in our calibration solutions was kept low (≤10 mM) to inhibit Na^+ gradient-dependent Mg^{2+} extrusion, possibly the main mechanism responsible for maintaining low $[Mg^{2+}]_i$ in this preparation (Nakayama et al., 1994; also see the companion article). Na^+ gradient across the cell membrane should be further dissipated by the application of monensin. 2) Very similar values of R were obtained at 49 mM $[Mg^{2+}]_o$ at various treatment times by the ionophores between 5 and 14 h. Because the tissue ATP was rapidly depleted during this period (Table 1), the estimate of R appears to be independent of the cellular ATP level. This implies that the contribution of ATP-driven Mg^{2+} pump on the cellular Mg^{2+} extrusion during the calibration runs is minor, if at all.

Another possibility is that the influence of protein binding has been underestimated in skeletal muscle fibers injected with a large amount of concentrated solutions (Westerblad and Allen, 1992). This maneuver should cause a large change in intracellular tonicity, which would result in water movement into the cell leading to cell swelling. In this situation, the influence of the indicator binding might be underestimated, because the dilution of the myoplasm might reduce the degree of the indicator binding to proteins, as discussed by Westerblad and Allen (1996).

Alternatively, the difference in intracellular alteration of R_{max} could simply reflect the difference in cell types (skeletal versus smooth muscles). Furaptra might bind to different proteins with a different degree in skeletal and smooth muscle cells, with the consequence that R_{max} is altered differently in these two tissues. To test this possibility, it would be necessary to apply two calibration methods to the same preparation under identical experimental conditions.

The finding of the somewhat larger furaptra K_D (for Mg^{2+}) in the cells than in salt solutions is consistent with the reported increase in K_D (for Ca^{2+}) of many Ca^{2+} indicators by binding to proteins (Konishi et al., 1988; Harkins et al., 1993; Kurebayashi et al., 1993; Baker et al., 1994). In the case of furaptra, it has been suggested, from the measurement of the Ca^{2+} transient with furaptra, that intracellular K_D for Ca^{2+} may be approximately twofold greater in frog skeletal muscle fibers than that in salt solutions (Konishi et al., 1991). For the furaptra-Mg^{2+} reaction, Konishi et al. (1993) assumed an analogous (twofold) increase in furaptra's K_D for Mg^{2+} in the frog myoplasm. The 46% increase in furaptra K_D for Mg^{2+} found in the present study is smaller than the 100% assumed by Konishi et al. (1993), and is slightly larger than the 21% reported by Westerblad and Allen (1992).

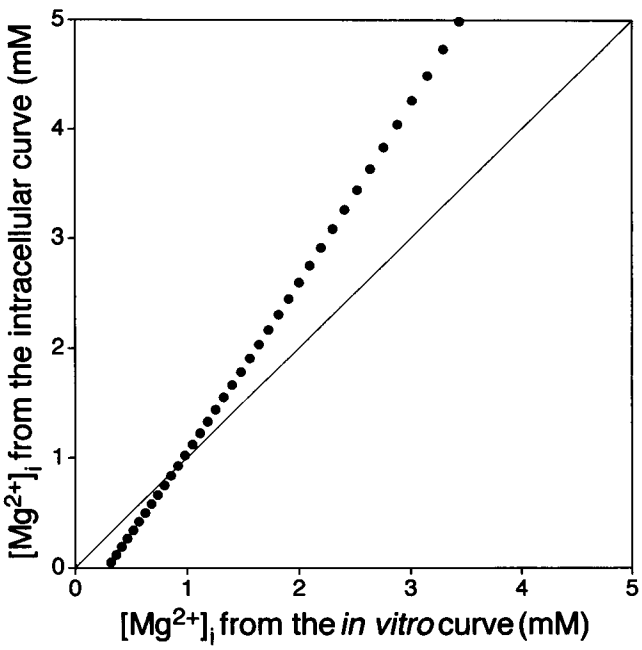

FIGURE 7 Comparison of estimates of $[Mg^{2+}]_i$ with the intracellular and the in vitro calibration curves shown in Fig. 6. For R ranging from 0.61 to 0.98 (0.01 step), the $[Mg^{2+}]_i$ calculated with the intracellular calibration curve after ΔR_{jump} correction (*ordinate*) was plotted against that calculated with the in vitro curve without ΔR_{jump} correction (*abscissa*). The straight line indicates agreement of $[Mg^{2+}]_i$ values calculated with both methods.

Basal $[Mg^{2+}]_i$ in tenia cecum

With the intracellular calibration curve (Fig. 6) and the R values, measured in normal Tyrode's solution and corrected for ΔR_{jump}, the basal $[Mg^{2+}]_i$ was calculated to be, on average, 0.98 mM (Table 2). We consider that this value is our best estimate of the basal $[Mg^{2+}]_i$ in tenia cecum at 25°C. On the other hand, the more commonly used method, in vitro calibration without correction for the ΔR_{jump}, yielded a very similar estimate of basal $[Mg^{2+}]_i$ averaging 0.95 mM (Table 2). Fig. 7 compares the two estimates of $[Mg^{2+}]$ with intracellular (*ordinate*) and in vitro (*abscissa*) calibrations at various $[Mg^{2+}]_i$ levels. It is clear that the two estimates coincide at ~0.9 mM. The estimate of basal $[Mg^{2+}]_i$ is, therefore, ~1.0 mM independent of the choice of the calibration method. The in vitro calibration will either underestimate or overestimate the $[Mg^{2+}]_i$ at concentrations higher or lower than 0.9 mM, respectively. The use of the intracellular calibration, therefore, becomes progressively important as the $[Mg^{2+}]_i$ is either elevated or lowered from its basal level (cf. Tashiro and Konishi, 1997).

The basal $[Mg^{2+}]_i$ level of ~1 mM estimated above may be compared with values reported from ^{31}P-NMR studies in smooth muscles. Kushmerick et al. (1986) obtained 0.40 mM and 0.46 mM as the estimates of basal $[Mg^{2+}]_i$ in rabbit uterine and urinary bladder smooth muscles, respectively (24°C). $[Mg^{2+}]_i$ values of 0.3–0.4 mM have also been estimated in tenia cecum of the guinea pig, the same tissue as used in the present study, at 32°C (Nakayama et al., 1994). At this point, we cannot provide a clear explanation for the discrepancy between our estimate of $[Mg^{2+}]_i$ and two to threefold lower value measured with ^{31}P-NMR. One disadvantage of the furaptra method is its sensitivity for Ca^{2+} (K_D for Ca^{2+} ~50 μM). At the basal $[Ca^{2+}]_i$ level normally encountered in the cytoplasm (<0.3 μM), the Ca^{2+} binding is considered to be negligible (<0.03 mM if calibrated as $[Mg^{2+}]_i$). However, if a substantial fraction of cells in the tissue is damaged possibly during the dissection process, elevated $[Ca^{2+}]_i$ could cause a change in R (Konishi et al., 1991; Hurley et al., 1992; Konishi and Berlin, 1993), which leads to an overestimation of $[Mg^{2+}]_i$. This could be the reason that, in some preparations (see Results), perfusion of the Ca^{2+}-free Tyrode's solution caused a detectable increase in R (apparent decrease in $[Mg^{2+}]_i$). We therefore estimated $[Mg^{2+}]_i$ only from preparations that showed little change in R (<0.01) upon removal of extracellular Ca^{2+}.

$[Mg^{2+}]_i$ measurements by ^{31}P-NMR, on the other hand, usually rely on the small chemical shift difference between α- and β-ATP resonances (for review, see London, 1991). Because Mg^{2+} binding to ATP approaches saturation (85–90%) at basal level of $[Mg^{2+}]_i$, the accuracy of $[Mg^{2+}]_i$ estimation may be limited by a small signal size. Clarke et al. (1996) proposed that the use of peak height ratio of the β- and α-ATP resonances, rather than chemical shift difference, could provide a more sensitive measure of $[Mg^{2+}]_i$. For the same ^{31}P-NMR spectra measured in working rat heart, they obtained an ~2-fold higher estimate of $[Mg^{2+}]_i$ using β- and α-ATP peak height ratio than that using the chemical shift difference.

Basal $[Mg^{2+}]_i$ in A7r5 cells and cardiac myocytes

The $[Mg^{2+}]_i$ estimated with the in vitro calibration (without ΔR_{jump} correction) was 0.70 mM in A7r5 cells, and 0.95 mM in rat cardiac myocytes (Table 2). With furaptra fluorescence calibrated in salt solutions, similar values of the $[Mg^{2+}]_i$ have been reported in cultured aortic smooth muscle cells (0.63 mM; Zhang et al., 1992; Ng et al., 1992) and rat cardiac myocytes (0.67 mM, Hongo et al., 1994; 0.82 mM, Handy et al., 1996). In mammalian cardiac myocytes, the basal $[Mg^{2+}]_i$ of ~1 mM has been estimated with other methods, including an ion-sensitive microelectrode with ETH-5214 (0.85 mM, Buri and McGuigan, 1990), ^{19}F-NMR (1.2 mM, Kirschenlohr et al., 1988; 0.85 mM, Murphy et al., 1989), mag-indo-1 fluorescence with intracellular calibration similar to that used in the present study (1.0 mM, Silverman et al., 1994). Values reported with ^{31}P-NMR vary between 0.4 mM and 1.4 mM (e.g., Kushmerick et al., 1986; Jalicks and Gupta, 1991; Nishimura et al., 1993).

Under the assumption that the intracellular calibration parameters obtained in tenia cecum could be directly applied to A7r5 cells and rat cardiac myocytes, the basal $[Mg^{2+}]_i$ calculated with the intracellular calibration curve in these cells was 0.7–1.1 mM, that is in close agreement with the values obtained with the in vitro calibration (Table 2). However, the intracellular estimates of $[Mg^{2+}]_i$ from these cells should be viewed with caution, because the intracellular calibration parameters might be different in different types of cells (see above).

The intracellular calibration method used in the present study should be applicable to other Mg^{2+} indicators in other types of preparations, if the preparations can be kept stable for a period of time long enough to reach $[Mg^{2+}]$ equilibrium (2 to 5 h). The present results revealed two potential sources of error in the use of ionophores to calibrate intracellular furaptra loaded with its AM form. Since similar problems likely exist in other ion indicators in cells other than smooth muscle, the technical approaches used here should be helpful to characterize these indicator problems in other preparations. The basal $[Mg^{2+}]_i$ was estimated to be ~1 mM in smooth muscle cells of tenia cecum (and ~0.7 mM in A7r5 cells), suggesting that $[Mg^{2+}]_i$ level of at least some types of smooth muscle cells might not be significantly lower than that in cardiac and skeletal muscle cells.

We thank S. Kurihara and S. Nakayama for helpful comments on the manuscript, Y. Ishida and T. Shibasaki for providing help on the measurement of tissue ATP content, M. Watanabe for advice on dissection of the tenia preparation, K. Hongo for providing single isolated myocytes, and N. Tomizawa for cell culture. We also thank M. Sibuya for reading the manuscript.

This work was supported by a Grant-in-Aid for Scientific Research from the Ministry of Education, Science, and Culture, Japan (to M.K.).

REFERENCES

Baker, A. J., R. Brandes, J. H. M. Schreur, S. A. Camacho, and M. W. Weiner. 1994. Protein and acidosis alter calcium-binding and fluorescence spectra of the calcium indicator indo-1. *Biophys. J.* 67: 1646–1654.

Baylor, S. M., S. Hollingworth, C. S. Hui, and M. E. Quinta-Ferreira. 1986. Properties of the metallochromic dyes Arsenazo III, Antipyrylazo III, and Azo 1 in frog skeletal muscle fibres at rest. *J. Physiol. (Lond.)* 377:89–141.

Blatter, L. A. 1990. Intracellular free magnesium in frog skeletal muscle studied with a new type of magnesium-selective microelectrode: interactions between magnesium and sodium in the regulation of $[Mg]_i$. *Pflügers Arch.* 416:238–246.

Buri, A., and J. A. S. McGuigan. 1990. Intracellular free magnesium and its regulation studied in isolated ferret ventricular muscle with ion-selective microelectrodes. *Exp. Physiol.* 75:751–761.

Butler, T. M., and R. E. Davies. 1980. High-energy phosphates in smooth muscle. *In* Handbook of Physiology, Sect. 2. The Cardiovascular System. C. N. Bohr, A. P. Somlyo, and V. S. J. Harvey, editors. Williams & Wilkins, Baltimore. 237–252.

Clarke, K., Y. Kashiwaya, M. T. King, D. Gates, C. A. Keon, H. R. Cross, G. K. Radda, and R. V. Veech. 1996. The β/α peak height ratio of ATP. A measure of free $[Mg^{2+}]$ using ^{31}P NMR. *J. Biol. Chem.* 271: 21142–21150.

Deber, C. M., J. Tom-kun, E. Mack, and S. Grinstein. 1985. Bromo-A23187: a nonfluorescent calcium ionophore for use with fluorescent probes. *Anal. Biochem.* 146:349–352.

Flatman, P. W. 1984. Magnesium transport across cell membranes. *J. Membr. Biol.* 80:1–14.

Handy, R. D., I. F. Gow, D. Ellis, and P. W. Flatman. 1996. Na-dependent regulation of intracellular free magnesium concentration in isolated rat ventricular myocytes. *J. Mol. Cell. Cardiol.* 28:1641–1651.

Harkins, A. B., N. Kurebayashi, and S. M. Baylor. 1993. Resting myoplasmic free calcium in frog skeletal muscle fibers estimated with fluo-3. *Biophys. J.* 65:865–881.

Hongo, K., M. Konishi, and S. Kurihara. 1994. Cytoplasmic free Mg^{2+} in rat ventricular myocytes studied with the fluorescent indicator furaptra. *Jpn. J. Physiol.* 44:357–378.

Hurley, T. W., M. P. Ryan, and R. W. Brinck. 1992. Changes of cytosolic Ca^{2+} interfere with measurements of cytosolic Mg^{2+} using mag-fura-2. *Am. J. Physiol.* 263:C300–C307.

Ishijima, S., T. Sonoda, and M. Tatibana. 1991. Mitogen-induced early increase in cytosolic free Mg^{2+} concentration in single Swiss 3T3 fibroblasts. *Am. J. Physiol.* 261:C1074–C1080.

Itoh, T., Y. Kanmura, and H. Kuriyama. 1985. A23187 increases calcium permeability of store sites more than of surface membranes in the rabbit mesenteric artery. *J. Physiol. (Lond.).* 359:467–484.

Jalicks, L. A., and R. K. Gupta. 1991. Intracellular free magnesium and high energy phosphates in the perfused normotensive and spontaneously hypertensive rat heart. A ^{31}P-NMR study. *Am. J. Hypertens.* 4:131–136.

Kirschenlohr, H. L., J. C. Metcalfe, P. G. Morris, G. C. Rodrigo, and G. A. Smith. 1988. Ca^{2+} transient, Mg^{2+}, and pH measurements in the cardiac cycle by ^{19}F-NMR. *Proc. Natl. Acad. Sci. USA.* 85:9017–9021.

Kishimoto, T., H. Ozaki, H. Karaki, N. Urakawa, and Y. Ishida. 1982. The inhibitory effect of monensin on high K-induced contraction in guinea-pig taenia coli. *Eur. J. Pharmacol.* 84:25–32.

Konishi, M., and J. R. Berlin. 1993. Ca transients in cardiac myocytes measured with a low-affinity fluorescent indicator, furaptra. *Biophys. J.* 64:1331–1343.

Konishi, M., S. Hollingworth, and A. B. Harkins, and S. M. Baylor. 1991. Myoplasmic calcium transients in intact frog skeletal muscle fibers monitored with the fluorescent indicator furaptra. *J. Gen. Physiol.* 97: 271–301.

Konishi, M., A. Olson, S. Hollingworth, and S. M. Baylor. 1988. Myoplasmic binding of fura-2 investigated by steady-state fluorescence and absorbance measurements. *Biophys. J.* 54:1089–1104.

Konishi, M., N. Suda, and S. Kurihara. 1993. Fluorescence signals from the Mg^{2+}/Ca^{2+} indicator furaptra in frog skeletal muscle fibers. *Biophys. J.* 64:223–239.

Kurebayashi, N., A. B. Harkins, and S. M. Baylor. 1993. Use of fura red as an intracellular calcium indicator in frog skeletal muscle fibers. *Biophys. J.* 64:1934–1960.

Kushmerick, M. J., P. F. Dillon, R. A. Meyer, T. R. Brown, J. M. Krisanda, and H. L. Sweeney. 1986. ^{31}P-NMR spectroscopy, chemical analysis, and free Mg^{2+} of rabbit bladder and uterine smooth muscle. *J. Biol. Chem.* 261:14420–14429.

Lardy, H. A., D. Johnson, and W. C. McMurray. 1958. Antibiotics as tools for metabolic studies. I. A survey of toxic antibiotics in respiratory, phosphorylative, and glycolic systems. *Arch. Biochem. Biophys.* 78: 587–597.

Levy, L. A., E. Murphy, B. Raju, and R. E. London. 1988. Measurement of cytosolic free magnesium ion concentration by ^{19}F-NMR. *Biochemistry.* 27:4041–4048.

Li, Q., R. A. Altschuld, and B. T. Stokes. 1987. Quantitation of intracellular free calcium in single adult cardiomyocytes by fura-2 fluorescence microscopy: calibration of fura-2 ratios. *Biochem. Biophys. Res. Commun.* 147:120–126.

London, R. E. 1991. Methods for measurement of intracellular magnesium: NMR and fluorescence. *Annu. Rev. Physiol.* 53:241–258.

Martell, A. E., and R. M. Smith. 1974. Critical Stability Constants, Vol. 1. Amino Acids. Plenum Publishing Corp., New York. 199–269.

Murphy, E., C. Steenbergen, L. A. Levy, B. Raju, and R. E. London. 1989. Cytosolic free magnesium levels in ischemic rat heart. *J. Biol. Chem.* 264:5622–5627.

Nakayama, S., H. Nomura, and T. Tomita. 1994. Intracellular-free magnesium in the smooth muscle of guinea pig taenia caeci: a concomitant analysis for magnesium and pH upon sodium removal. *J. Gen. Physiol.* 103:833–851.

Ng, L. L., J. E. Davies, and M. Ameen. 1992. Intracellular free-magnesium levels in vascular smooth muscle and striated muscle cells of the spontaneously hypertensive rat. *Metabolism.* 41:772–777.

Nishimura, H., T. Matsubara, Y. Ikoma, S. Nakayama, and N. Sakamoto. 1993. Effects of prolonged application of isoprenaline on intracellular free magnesium concentration in isolated heart of rat. *Br. J. Pharmacol.* 109:443–448.

Raju, B., E. Murphy, L. A. Levy, R. D. Hall, and R. E. London. 1989. A fluorescent indicator for measuring cytosolic free magnesium. *Am. J. Physiol.* 256:C540–C548.

Reed, P. W., and H. A. Lardy. 1972. A23187: a divalent cation ionophore. *J. Biol. Chem.* 247:6970–6977.

Silverman, H. S., F. D. Lisa, R. C. Hui, H. Miyata, S. J. Sollott, R. G. Hansford, E. G. Lakatta, and M. D. Stern. 1994. Regulation of intracellular free Mg^{2+} and contraction in single adult mammalian cardiac myocytes. *Am. J. Physiol.* 266:C222–C233.

Somlyo, A. P., A. V. Somlyo, H. Shuman, and M. Endo. 1982. Calcium and monovalent ions in smooth muscle. *Fed. Proc.* 41:2883–2890.

Strehler, B. L., and W. D. McElroy. 1957. Assay of adenosine triphosphate. *In* Methods in Enzymology. S. P. Colowick and N. O. Kaplan, editors. Academic Press, New York. 871–873.

Tashiro, M., and M. Konishi. 1997. Na^+ gradient-dependent Mg^{2+} transport in smooth muscle cells of guinea pig tenia cecum. *Biophys. J.* 73:3371–3384.

Tashiro, M., M. Konishi, and S. Kurihara. 1996a. Intracellular calibration of the Mg^{2+} indicator furaptra in smooth muscle cells of guinea-pig taenia caecum. *J. Muscle Res. Cell Motil.* 17:291.

Tashiro, M., M. Konishi, and S. Kurihara. 1996b. Intracellular Mg^{2+} concentration of smooth muscle cells measured with fluorescent indicator furaptra. *Jpn. J. Physiol.* 46:S82.

Tashiro, M., M. Konishi, and S. Kurihara. 1997. Fluorescence signal of the Mg^{2+} indicator furaptra (mag-fura-2) calibrated in guinea pig taenia caeci. *Biophys. J.* 72:185*a* (Abstr.).

Westerblad, H., and D. G. Allen. 1992. Myoplasmic free Mg^{2+} concentration during repetitive stimulation of single fibres from mouse skeletal muscle. *J. Physiol. (Lond.).* 453:413–434.

Westerblad, H., and D. G. Allen. 1996. Intracellular calibration of the calcium indicator indo-1 in isolated fibers of Xenopus muscle. *Biophys. J.* 71:908–917.

Williams, D. A., and F. S. Fay. 1990. Intracellular calibration of the fluorescent calcium indicator Fura-2. *Cell Calcium.* 11:75–83.

Yamamoto, H., and C. van Breemen. 1986. Ca^{2+} compartments in saponin-skinned cultured vascular smooth muscle cells. *J. Gen. Physiol.* 87:369–389.

Zhang, A., T. P.-O. Cheng, B. T. Altura, and B. M. Altura. 1992. Extracellular magnesium regulates intracellular free Mg^{2+} in vascular smooth muscle cells. *Pflügers Arch.* 421:391–393.